4th International Conference on the Durability of Concrete Structures
24–26 July 2014
Purdue University, West Lafayette, IN, USA

Saturation of Air Entrained Voids and Its Implication on the Transport of Ionic Species in Concrete

Yiwen Bu
School of Materials Engineering, Purdue University

Jason Weiss
Lyles School of Civil Engineering, School of Materials Engineering, Purdue University

ABSTRACT

Air entrainment is commonly used to improve the durability of concrete materials exposed to freezing and thawing. While the influence of air voids on freeze/thaw damage and salt scaling is frequently studied, the influence of entrained air voids on ionic transport has been studied less frequently. Since ionic transport in concrete materials relies on pore fluid as the medium of conduction, only saturated or partially saturated air voids participate in the transport processes. This paper discusses the conditions under which air voids could become saturated. Specifically, the saturation condition of entrained air voids in laboratory tests and in service is discussed. This paper compares the results of steady and non-steady state migration tests on concrete specimens when air voids are saturated and when air voids are primarily empty. The implications of the observed difference are discussed to provide a better understanding of the direct application of laboratory test results to predict the service life of concrete materials in the field. The saturation of air voids is observed to also influence the electrical resistivity of concrete materials.

1. INTRODUCTION

Concrete used in service is commonly air-entrained to increase the durability when exposed to a freeze and thaw environment. The entrained air voids are typically 10–500 μm in diameter and constitute 1–8% of the volume of the fresh concrete. The air voids are usually larger than the capillary pores [10 nm to 10 μm (Mindess, Young, & Darwin, 2003)] of the cementitious systems, and ideally are isolated from each other but connected with the capillary pore systems of the cementitious matrix (Litvan, 1988; Sutter, Van Dam, & Thomas, 2007). Entrained air voids that remain unsaturated in service can release pressure for the expansive ice formation under the freezing temperature (Fagerlund, 1977; Farnam, Bentz, Sakulich, Flynn, & Weiss, 2014; Li, Pour-Ghaz, Castro, & Weiss, 2012; Pinto & Hover, 2001).

The corrosion of reinforcing bars due to chloride ingress is an additional cause for the degradation of concrete structures (Bentur, Diamond, & Berke, 1998; Liu & Weyers, 1998). Chloride ingress relies on pore fluid as the transport medium; therefore when entrained air voids are saturated or partially saturated, they could become paths of chloride transport. However, Li et al. estimated that even in thin sections it may take 3–6 years for air-entrained concrete materials to reach a critical degree of saturation (DOS) under continuous exposure to water (Li et al., 2012). Thus it is possible that concrete materials in service may have most of the air voids unfilled. On the other hand, various laboratory tests to assess the rate of chloride ingress may be performed when the entrained air voids are partially or fully saturated, such as ASTM C1556-11, ASTM C1202-10, and Stadium® ionic diffusion coefficient (IDC) tests (SIMCO Technologies Inc., 2013). Vacuum saturation (under a pressure of ≤50 Torr) is used in these tests and it was observed that under a pressure of 7 ± 2 Torr, air voids can be mostly saturated (Bu, Spragg, & Weiss, 2014).

Since laboratory test results are becoming more frequently used to predict the service life of concrete materials in the field (Ehlen, Thomas, & Bentz, 2009; Samson & Marchand, 2007), the possibility of having different chloride transports in concrete materials when different levels of saturation are reached and when entrained air voids are at different degrees of saturation needs to be better understood. Wong, Pappas, Zimmerman, and Buenfeld (2011) estimated based on experimental data that for every 1% increase of air content, the IDCs decrease by 4% when the air voids are unsaturated.

This paper discusses the conditions under which the air voids could become partially or fully saturated. Steady and non-steady state migration tests were performed on concrete materials under two conditions: (1) when air voids are mostly saturated and (2) when air voids remain primarily empty. The saturation condition of the entrained air voids on the electrical resistivity of the concrete materials was also evaluated.

2. MATERIALS

Two concrete mixtures (w/c = 0.41 and 0.48) were prepared with air entrainment, and one mortar mixture (w/c = 0.30) was prepared with no air entrainment (Table 1). A Type I ordinary Portland cement (ASTM C150-12) was used with an estimated Bogue composition of 61% C_3S, 8% C_2S, 9% C_3A, 10% C_4AF, a Na_2O_{eq} of 0.86% and a Blaine fineness of 375 m^2/kg. The fine aggregate used had a specific gravity of 2.66 and an absorption capacity of 1.80%. The coarse aggregate used had a specific gravity of 2.74, an absorption capacity of 0.8%, and a nominal maximum aggregate size of 1″ (25.4 mm). Both concrete and mortar were cast in 4″ by 8″ (102 mm × 204 mm) cylindrical molds, vibrated, and rodded according to ASTM C192-07 and ASTM C305-13, respectively. All materials were cured sealed at 23 ± 1°C until the time of testing.

Table 1. Mixture proportions of test materials.

	Concrete		Mortar
w/c	0.41	0.48	0.30
Cement (kg/m³)	390.4	353.6	728.6
Water (kg/m³)	160.1	169.7	218.6
Fine aggregate (kg/m³)	735.7	698.9	1418.5
Coarse Aggregate (kg/m³)	1068.0	1056.0	–
Air (%)	6.2*	5.0*	–

*As measured in accordance with ASTM C231-10.

3. EXPERIMENTAL

3.1 Non steady-state migration tests

At the age of 6 months, concrete (w/c = 0.41) and mortar (w/c = 0.30), cylinders (102 mm × 204 mm) were demolded and cut in half to produce specimens that were 102 mm in diameter and 75 ± 1 mm in thickness by removing the ends off the cylinders. The specimens were coated with epoxy on all sides except the exposed surface. After the epoxy coating had hardened, half of the specimens were vacuum saturated (under 7 ± 2 Torr) with lime water and immersed in 165 g/L NaCl solution in accordance with ASTM C1556-11, while the other half were immersed directly (without applying the vacuum saturation) in 165 g/L NaCl solution. The ratio of exposure surface area to solution volume was kept constant as 54.4 cm^2/L (ASTM C1556-11).

Specimens were exposed to the NaCl solution for either 3 or 35 days. After immersion, specimens were removed from the solution, kept in a 23 ± 2°C, 50 ± 3% RH chamber for 24 ± 1 h. Powders were then ground layer by layer (in 1 mm steps) and dissolved in a nitric acid solution (Di Bella et al., 2012). The chloride contents were determined with an automated titrator for the first 1 mm at the surface, and every 2 mm thereafter (ASTM C1556-11). Background chloride content was also determined according to ASTM C1556-11. The experimental chloride profiles were fitted with solution of Fick's second law:

$$\frac{C_{x,t} - C_0}{C_s - C_0} = erfc\left(\frac{x}{2\sqrt{D_{APP}t}}\right) \quad (1)$$

where $C_{x,t}$ (% by weight)is the concentration of chloride ions at time t (s), at a distance x (m) from the exposure surface, C_0 is the background chloride concentration that is initially present in the concrete (% by weight), C_S is the surface chloride concentration (% by weight), D_{APP} is the apparent chloride diffusion coefficient (m^2/s), and erfc (y) is the complimentary error function of y.

3.2 Steady-state migration tests

The IDC test (SIMCO Technologies Inc., 2013) could be considered as a near steady-state migration testing technique due to the relatively large solution compartments (≈2.5 L) used and the longer testing duration (2 weeks) as compared to ASTM C1202-10. The test specimens are 50 ± 1 mm thick and coated on the circumference with epoxy. The downstream compartment is filled with a 300 mmol/L NaOH solution, while the upstream compartment is filled with a solution of 300 mmol/L NaOH and 500 mmol/L NaCl. The current that evolved under an external voltage supply of 10 V was recorded for the testing duration of 2 weeks. The temperature of the solution compartments was monitored and found to remain stable at 23 ± 1°C.

In this study, IDC tests were performed on both specimens where entrained air voids are primarily empty and specimens where entrained air voids are saturated. The specimens of the IDC tests are to be vacuum saturated (under a pressure of less than 50 Torr) with 300 mmol/L NaOH solution (SIMCO Technologies Inc., 2013) before the migration tests when the standard protocol is followed. The IDC test results were then simulated with Stadium® Lab V3.0, which does not account for advection of ions due to moisture gradients, to calculate the IDCs. For this reason, performing IDC tests on unsaturated specimens and subjecting the test results to the subsequent simulation can be problematic. However, the moisture gradients could be minimized if the pores in the cementitious matrix are saturated except for the air entrained voids, while the saturation of air voids is slow (Bu et al., 2014; Li et al., 2012) and should not cause substantial moisture flow during the test duration of 2 weeks.

To prepare specimens where the cementitious matrix was primarily saturated but the entrained air voids

were primarily empty, concrete specimens (w/c = 0.48) were cut to 50 ± 1 mm thickness (102 mm in diameter) and oven dried [since oven-drying increases the rate of water absorption (Castro, Bentz, & Weiss, 2011)]. The oven-dried specimens were allowed to cool to room temperature and were immersed in 300 mmol/L NaOH solutions for 7 days. At this point, the mass change of the specimens is less than 0.01% of the former mass during every 24 h. Specimens were then coated on the circumferences with epoxy and tested with IDC migration cells. The mass increase of the specimens during 2 weeks of testing was measured to be less than 1.0 g (less than 0.1% of the specimen mass). To be consistent, test specimens with both the cementitious matrix and the air voids saturated were also oven-dried before vacuum saturation (under a pressure of 7 ± 2 Torr) was performed. This was to ensure that any microstructural changes during drying were comparable for all specimens.

3.3 Porosity inputs for IDC tests

In addition to the test currents and voltages obtained from the IDC tests, a porosity input was necessary for the calculation of tortuosity in Stadium® Lab V3.0. The mass conservation equation (Samson & Marchand, 2007) behind the simulation indicates that the simulated tortuosity (τ) depends directly on the input of porosity (φ):

$$\frac{\partial(\phi c_i)}{\partial t} = div(D_0\tau\ \phi grad(c_i) + \frac{D_0\tau z_i F\phi}{RT} c_i grad(\psi) + D_0\tau\phi c_i grad(ln\gamma_i)) - \rho\frac{\partial c_i^b}{\partial t} \quad (2)$$

where c_i is the concentration of species i (mmol/L), t is the time variable (s), D_0 is the intrinsic diffusion coefficient of species i (m^2/s), z_i is the valence number of ionic species i, F is the Faraday constant, R is the gas constant, T is the absolute temperature (K), ψ is the electro-diffusion potential (V), γ_i is the activity coefficient, ρ is the density of the materials (kg/m^3), and C_i^b is the amount of physically bound species (mol/kg).

The porosity input could be subject to the testing methods. Even though, it is specified that this value should be obtained following ASTM C642-13 (SIMCO Technologies Inc., 2013), Bu et al. (2014) showed that the immersion and boiling method failed to saturate the large entrapped air voids and the entrained air voids in concrete materials, and thus, underestimated the total volume of permeable voids.[1] Vacuum saturation (under a pressure of 7 ± 2 Torr), however, filled in the air voids and provided a more reliable estimation of the total pore volumes.

1 However it provides a reasonable estimation of the pores in the matrix (excluding entrained air voids).

Therefore, it is believed that the input of porosity should be obtained by the same approach with which the test specimens are conditioned, only by which the porosity inputs correspond to the volume of pores that participate in the ionic diffusion/migration process. For this reason, porosity inputs for vacuum saturated specimens were obtained using vacuum saturation under the same pressure (7 ± 2 Torr). For specimens immersed for 7 days (specimens with entrained air voids primarily empty), the porosity inputs were the percent volume of pores that were filled after 7 days of immersion.

3.4 Electrical resistivity

The uniaxial electrical resistance was measured for oven-dried concrete specimens (w/c = 0.48) that were vacuum saturated (7 ± 2 Torr) with 300 mmol/L NaOH solution and oven-dried specimens that were simply immersed in the same solution. This solution was chosen instead of lime water to reduce the effect of alkali leaching on the measurements of electrical resistance (Bu & Weiss, 2014; Spragg et al., 2013). The equipment used for the uniaxial bulk resistance testing is a Miller-400D digital resistance meter, operating at voltage of 12 V and a frequency of 82.2 Hz, with an accuracy of ±0.01 Ω. A set of 4-inch diameter stainless steel plate electrodes was used with thin sponges. The sponges were wetted with the 300 mmol/L NaOH solution and placed between specimens and plate electrodes during testing to ensure a good electrical contact between the two. The electrical resistivity of concrete specimens were then calculated from the measured resistance with the methods described in Spragg, Castro, Nantung, Paredes, and Weiss, (2012).

4. RESULTS AND DISCUSSIONS

4.1 Non-steady-state migration tests

After 3 days of ponding, the chloride profiles indicate that for both concrete specimens (Figure 1) and mortar specimens (Figure 2), chloride ions penetrated deeper into specimens that were directly immersed in NaCl solutions than it did in the samples vacuum saturated before exposure. This could be explained by the greater advection of chloride ions due to moisture absorption in unsaturated specimens or the dilution effects in a solution with less fluid. It is also noticed that the total chloride content at each depth is lower for saturated specimens than unsaturated ones for non-entrained mortar. However, for air-entrained concrete specimens (w/c = 0.41), the chloride content at the surface layers is, instead, higher in saturated specimens than in unsaturated ones.

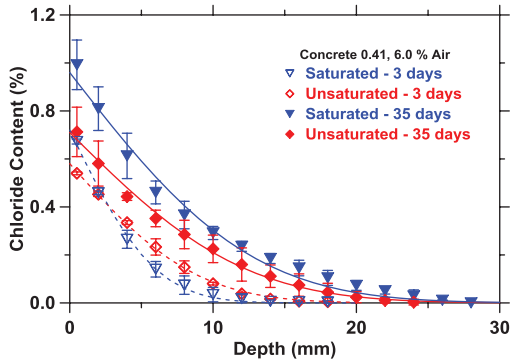

Figure 1. Chloride penetration profiles of concrete specimens (w/c = 0.41, saturated and unsaturated) subjected to 3 and 35 days of ponding in 165 g/L NaCl solution. Each data point is an average of three ponding specimens. Background chloride was subtracted from all chloride profiles. The solid and dotted lines are fitting with Equation (1).

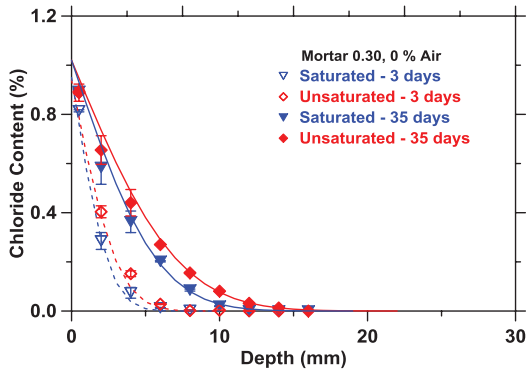

Figure 2. Chloride penetration profiles of mortar specimens (w/c = 0.30, saturated and unsaturated) subject to 3 and 35 days of ponding in 165 g/L NaCl solution. Each data point is an average of three ponding specimens. Background chloride was subtracted from all chloride profiles. The solid and dotted lines are fitting with Equation (1).

After 35 days of ponding, unsaturated mortar specimens with no air entrainment still showed further chloride ingress when compared with the saturated counterparts (Figure 2) and less total chloride contents at each depth. However, for concrete (w/c = 0.41) with air entrainment, unsaturated specimens showed instead a reduced penetration depth and reduced total chloride contents at each depth (Figure 1).

The chloride profiles are fitted with solution of Fick's second law [Equation (1)] to determine the surface chloride concentration (C_s) and the apparent chloride diffusion coefficients (D_{APP}) (Figures 1 2). Table 2 shows that the fitted C_s is similar for saturated and unsaturated mortar specimens after both 3 and 35 days of ponding. The fitted D_{APP} is greater for unsaturated mortar specimens after both ponding durations (3 and 35 days). This reflects the overall acceleration of chloride penetration speed since diffusion under a concentration gradient is coupled with advection due to a moisture gradient.

Table 2. Fitted surface chloride concentration (C_s) and apparent chloride diffusion coefficients (D_{APP}) for mortar specimens (w/c = 0.30).

Condition and ponding time	Mortar 0.30, Non air entrained	
	C_s (%)	D_{APP} (e^{-11} m²/s)
Unsaturated, 3 days	0.94 ± 0.035	1.14 ± 0.070
Saturated, 3 days	0.95 ± 0.046	0.73 ± 0.278
Unsaturated, 35 days	1.02 ± 0.056	0.52 ± 0.034
Saturated, 35 days	1.02 ± 0.043	0.34 ± 0.046

Table 3 shows the fitted C_s and D_{APP} for concrete specimens (w/c = 0.41) with air entrainment. It is noticed that for both ponding durations, C_s is greater (24% greater at 3 days and 33% greater at 35 days) for saturated specimens than for unsaturated specimens.

Table 3. Fitted surface chloride concentration (C_s) and apparent diffusion coefficients (D_{APP}) for concrete specimens (w/c = 0.41).

Condition and ponding time	Concrete 0.41, 6.0% air	
	C_s (%)	D_{APP} (e^{-11} m²/s)
Unsaturated, 3 days	0.58 ± 0.031	9.29 ± 1.378
Saturated, 3 days	0.72 ± 0.001	4.14 ± 1.228
Unsaturated, 35 days	0.71 ± 0.161	1.51 ± 0.165
Saturated, 35 days	0.96 ± 0.084	1.64 ± 0.113

To understand the reason for the difference in C_s (Table 3) between saturated and non-saturated concrete specimens, the total chloride content is divided into free chloride content in the pore solution and the amount of bound chloride by the solid phases. The free chloride content could be calculated from the free chloride concentration in the pore fluid and the volume of the pore fluid (Bu, Luo, Lin, & Weiss, 2013), while the amount of bound chloride depends on the chloride concentration in the pore fluid, the chloride binding phases, and the contact area (volume and sizes of pores filled) between the solid and liquid phases (Glass & Buenfeld, 2000; Luping & Nilsson, 1993; Spiesz, Ballari, & Brouwers, 2012).

Considering that the free chloride concentrations should be similar in the surface layers for both saturated and unsaturated specimens (the same 165 g/L NaCl solution was used), and so should the chloride binding phases, the free chloride and bound chloride could only be reduced (as in the case of unsaturated specimens) if there is a reduction in the pore fluid volume (and contact area between NaCl solution and the solid phases). Such reduction in the pore fluid volume was not due to a different total porosity, since the specimens are from the same mixture and at the same age. It is thus more likely that the larger pores in the unsaturated specimens cannot be filled with the ponding solutions even after 35 days of immersion

(Bu et al., 2014), resulting in less free chloride content and possibly less bound chloride. This is likely due to a lack of capillary suction in the relatively large air voids (10–500 μm).

The saturation of air voids also influence the fitted D_{APP}. After 3 days of ponding, D_{APP} is greater for unsaturated concrete specimens compared to saturated specimens (Table 4). This is due to the fact that the moisture gradient in unsaturated specimens accelerated the transport of chloride ions, especially near the surface. However, it is noticed that D_{APP} became similar for saturated specimens and unsaturated specimens after 35 days of ponding. During the 35-day ponding, it is likely that the influence of the absorption process is more significant in the first 7–10 days (Castro et al., 2011) when chloride ingress is accelerated by moisture gradient in unsaturated specimens. At later times, the moisture gradient becomes relatively insignificant, and the air voids remain primarily empty (as suggested by the reduction in C_s in unsaturated specimens after 35 days of ponding in Table 3). A reduction of diffusion coefficient may be observed in concrete materials with air voids empty (Wong et al., 2011). The overall speed of chloride ingress as reflected by D_{APP}, when "averaged" over these two periods therefore became similar for saturated and non-saturated specimens.

Table 4. Specimens conditioning corresponding porosity input and simulation results for saturated and unsaturated concrete specimens (w/c = 0.48).

Condition	Porosity input	Simulated tortuosity
Immersed	15.03%	0.0653
Vacuum Saturated (7 ± 2 Torr)	18.60%	0.0678
*Vacuum Saturated (7 ± 2 Torr)	*(ASTM) 15.50%	0.0792

*Conditioning method as specified by (SIMCO Technologies Inc., 2013).

As models are being designed to predict chloride ingress in unsaturated concrete materials subject to both ionic concentration gradient and moisture gradient (Ehlen et al., 2009; Olsson, Baroghel-Bouny, Nilsson, & Thiery, 2013; Samson & Marchand, 2007), the fact that air voids (10–500 μm) are not as easily filled as most capillary pores (10 nm to 10 μm) should be considered, as this directly alters the determination of chloride content at each depth, and thus, the time of corrosion initiation. The reduced chloride diffusion coefficients when air voids are empty should also be investigated and accounted for.

4.2 Steady-state migration tests

The concrete specimens (w/c = 0.48) for IDC tests were prepared by oven-drying the specimens first. Subsequently, half of the specimens were immersed in 300 mmol/L NaOH solution and mass gain of the specimens was recorded over time. The other half of the oven-dried specimens were vacuum saturated under a pressure of 7 ± 2 Torr. Figure 3 shows that specimens that were vacuum saturated (18 ± 2 h) gained more mass than specimens that are simply immersed even after 2 months of immersion.

The rate of mass gain for immersed specimens is more significant in the first 7 days, during which period pores excluding air voids are preferentially filled due to the greater capillary suction. Assuming a degree of hydration (DOH) of 81% (measured with loss on ignition on paste specimens (w/c = 0.48) at 6 months), the theoretical porosity [using Power's model (Jensen & Hansen, 2001)] of the concrete materials excluding air voids are 15.1% (matrix porosity = 12.9%, aggregate porosity = 2.2%). To fill these pores in the test specimens (102 mm × 50 mm) needs 62.9 g of 300 mmol/L NaOH solution (density = 1.012 g/cm^3). This is similar to the mass gain of the immersed test specimens at the end of 7 days (Figure 3). The air voids, therefore, are likely not filled in after 7 days of immersion and are slowly filled in at later times. Vacuum saturation (under 7 ± 2 Torr), instead, was able to fill in these air voids in the relatively short duration of 18 ± 2 h and result in a total mass gain of 77 g. The difference between mass gain after vacuum saturation (77 g) and mass gain after 7 days of immersion (62.9 g) is the mass of NaOH solution held in the entrapped and entrained air voids. This corresponds to a 3.6% of air content in hardened concrete. This is less than the 5.0% as measured in fresh concrete (Table 1); however, such reduction could be due to loss of air during specimen preparation (AASHTO T152-13-UL, 2013).

The vacuum saturated (7 ± 2 Torr) specimens (with 300 mmol/L NaOH solution) and the specimens immersed for 7 days in the same solution were tested

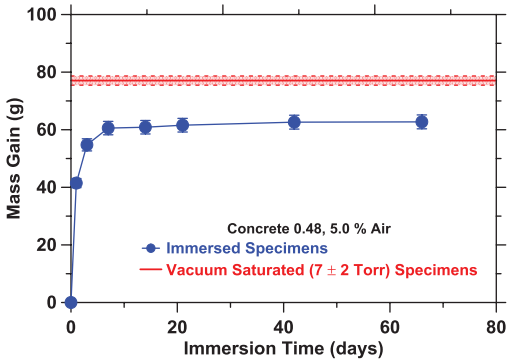

Figure 3. Mass gain for specimens conditioned for IDC tests. Each data point is an average of three specimens. Standard deviations are indicated with error bars (immersed specimens) or line width (vacuum saturated specimens).

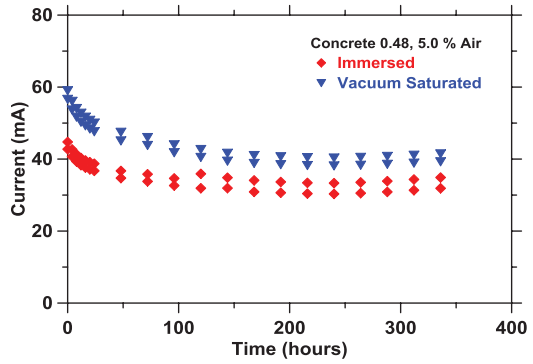

Figure 4. IDC test currents for saturated and unsaturated concrete specimens (w/c = 0.48).

with IDC migration cells. Figure 4 shows that during the testing duration of 2 weeks, a lower current is observed for immersed specimens. This indicates a greater electrical resistance of concrete specimens when air voids are not saturated compared to specimens when air voids are saturated. The total charge passed (the area under the current verses time plot) over the test duration of 2 weeks is also less for immersed specimens than for vacuum saturated specimens. Similar observations on total charges passed may also be observed in rapid chloride penetration tests (ASTM C1202-10) if performed on these specimens.

The test currents and voltages are simulated to derive the tortuosity of the specimens. The simulation results are shown in Table 3. The porosity inputs are different for immersed (15.03%) and vacuum saturated specimens (18.60%) due to the different volume of pores that were filled with the 300 mmol/L NaOH solution, and thus, participated in ionic transport (explained also in Section 3.3). The simulated tortuosity obtained are, however, similar for both specimen conditioning, with the unsaturated specimens having slightly lower tortuosity [lower IDCs (Samson & Marchand, 2007)].

In addition, simulations were also performed for vacuum saturated specimens with the input of porosity measured following ASTM C642-13, in accordance with (SIMCO Technologies Inc., 2013). The ASTM porosity (15.50%) is higher than the percent volume of pores filled with immersion (15.03%) due to the additional boiling of the specimens. Nonetheless, even after boiling, the air voids are still not completely filled, considering that 15.50% is still lower than porosity measurements obtained with vacuum saturation (18.60%).

The simulated tortuosity for vacuum saturated specimens with the input of ASTM porosity is 16.8% higher than the simulated tortuosity with the input of percent pore volume obtained with vacuum saturation. This is related to the porosity input (15.50%) that underestimated the total volume of pore fluid (18.60%) that participates in ionic transport. Equation 2 suggests that porosity and tortuosity are directly related parameters and thus the incorrect estimation of one will lead to an incorrect calculation of the other.

4.3 Electrical resistivity

The electrical resistivity of the concrete specimens decreased as the air voids become slowly filled during 7–67 days of immersion (Figure 5). The resistivity of the specimens after 67 days of immersion decreased by 5% compared to specimens after 7 days of immersion. When air voids were primarily filled (vacuum saturated at 7 ± 2 Torr) the resistivity of the specimens decreased by more than 25% compared to specimens immersed for 7 days. This is consistent with the greater migration test currents as shown in Figure 4 for vacuum saturated specimens than for immersed specimens.

To quantify the relationship between saturation of air voids and the electrical resistivity of the specimens, a saturation function *f*(S*)* proposed by Weiss, Snyder, Bullard, and Bentz (2013) was used:

$$\frac{\rho_c^o}{\rho_c} = f(S) = S^n \tag{3}$$

where ρ_c^0 is the resistivity of the concrete materials at complete saturation, *S* is the DOS (the percentage of the total pore volume that is filled with fluid), ρ_c is the resistivity of the concrete materials at any DOS, and *n* is an empirical component that depends on the pore structure of the materials.

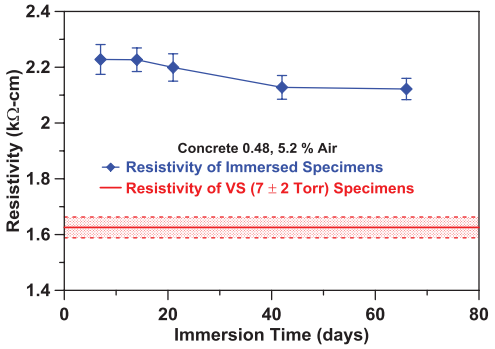

Figure 5. Decrease of electrical resistivity as air voids in immersed specimens being filled (in 300 mmol/L NaOH solution) over time and the resistivity of specimens vacuum saturated (VS) (7 ± 2 Torr) with the same solution. Each data point is an average of three specimens.

Figure 6 shows that as the degree of saturation (*S*) is increasing due to the infilling of the air voids, a value of *n* = 1.5 fits the data reasonably. This value of *n* is lower than the typical range of 3–6 for mortar materials (Weiss et al., 2013). However, this is likely caused

by the coarser size of the air voids (10–500 μm) as compared to the capillary pores (10 nm to 10 μm) of the cementitious system and a lack of "ink-bottle" shaped air-voids. As an example, for porous rocks such as siltstone, *n* is observed to be 2 due to a coarser and more open pore structure (Weiss et al., 2013).

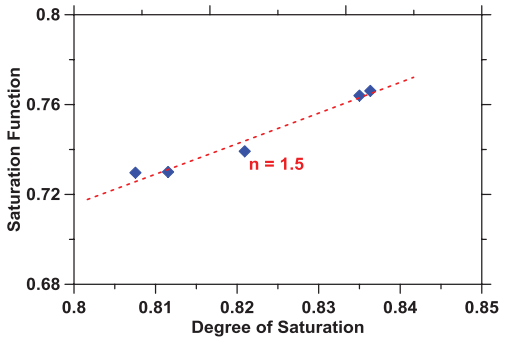

Figure 6. Saturation function during the infilling of air voids in immersed specimens (in 300 mmol/L NaOH solution).

5. CONCLUSIONS

The saturation of air voids in the concrete materials is not easily achieved with immersion and boiling method as described in ASTM C642-13. However, it can be achieved using a sufficient level of vacuum saturation of 7 ± 2 Torr.

When ponding tests were performed on unsaturated concrete materials with air entrainment (measured as 6.2% for fresh concrete), the air voids remain primarily unsaturated after 35 days of ponding and resulted in a 25% decrease of fitted surface chloride concentration when compared with saturated samples.

Concrete specimens with unsaturated air voids showed 25% lower currents (under similar voltages) during the steady-state migration tests (Stadium® IDC tests), and would result in reduced total charge passed in the rapid chloride penetration test (ASTM C1202-10). Specimens with empty entrained air voids showed a slight decrease of pore tortuosity and a slight decrease of IDCs.

Concrete specimens with unsaturated air voids (measured as 5.0% for fresh concrete) showed approximately 25% increase in electrical resistivity compared to completely saturated specimens. The electrical resistivity of the concrete materials when only air voids are unsaturated could be related to that of a completely saturated specimen with a saturation function $f(s) = s^{1.5}$.

ACKNOWLEDGMENTS

This work was supported in part by the Joint Transportation Research Program administered by the Indiana Department of Transportation and Purdue University under SPR 3280. The work described in this paper was conducted in the Pankow Laboratory at Purdue University, and the authors would like to acknowledge the support that has made its operation possible. The contents of this paper reflect the views of the authors, who are responsible for the facts and the accuracy of the data presented herein, and do not necessarily reflect the official views or policies of the Federal Highway Administration and the Indiana Department of Transportation, nor do the contents constitute a standard specification or regulation.

REFERENCES

AASHTO T152-13-UL. (2013). Standard method of test for air content of freshly mixed concrete by the pressure method. *American Association of State Highway and Transportation Officials.*

Bentur, A., Diamond, S., & Berke, N. (1998). *Steel corrosion in concrete*. London, England: CRC Press.

Bu, Y., Luo, D., Lin, B., & Weiss, W. J. (2013). Chloride ingress in concrete in different NaCl concentrations: Comparing Fick's second law & Nernst—Planck approaches. In *Proceedings of 33rd Cement and Concrete Science Conference*. Portsmouth, UK.

Bu, Y., Spragg, R., & Weiss, W. J. (2014). Comparison of the pore volume in concrete as determined using ASTM C642 and vacuum saturation. *Advances in Civil Engineering Materials*, In press.

Bu, Y., & Weiss, J. (2014). The influence of alkali content on the electrical resistivity and transport properties of cementitious materials. *Cement and Concrete Composites, 51,* 49–58.

Castro, J., Bentz, D., & Weiss, J. (2011). Effect of sample conditioning on the water absorption of concrete. *Cement and Concrete Composites, 33*(8), 805–813.

Ehlen, M., Thomas, M., & Bentz, E. (2009, May). Life-365 Service Life Prediction Model™ Version 2.0. *Concrete International, 31*(5), 41–46.

Fagerlund, G. (1977). The international cooperative test of the critical degree of saturation method of assessing the freeze/thaw resistance of concrete. *Matériaux et Constructions, 10*(4), 231–253.

Farnam, Y., Bentz, D. P., Sakulich, A., Flynn, D., & Weiss, J. (2014). Measuring freeze and thaw damage in mortars containing deicing salt using a low temperature longitudinal guarded comparative calorimeter and acoustic emission (AE-LGCC). *Advances in Civil Engineering Materials, 3*(1), 1–22.

Glass, G. K., & Buenfeld, N. R. (2000). The influence of chloride binding on the chloride induced corrosion risk in reinforced concrete. *Corrosion Science, 42*(2), 329–344.

Jensen, O. M., & Hansen, P. F. (2001). Water-entrained cement-based materials. *Cement and Concrete Research, 31*(4), 647–654.

Li, W., Pour-Ghaz, M., Castro, J., & Weiss, J. (2012). Water absorption and critical degree of saturation relating to freeze-thaw damage in concrete pavement joints. *Journal of Materials in Civil Engineering, 24*(3), 299–307.

Litvan, G. G. (1988). The mechanism of frost action in concretetheory and practical implications. In *Proceedings of Workshop on Low Temperature Effects on Concrete*, National Research Council of Canada, Montreal, Canada, 115–134.

Liu, Y., & Weyers, R. (1998). Modelling the time-to-corrosion cracking in chloride contaminated reinforced concrete structures. *ACI Materials Journal, 95*, 675–681.

Luping, T., & Nilsson, L.-O. (1993). Chloride binding capacity and binding isotherms of OPC pastes and mortars. *Cement and Concrete Research, 23*(2), 247–253.

Mindess, S., Young, J., & Darwin, D. (2003). *Concrete*. Upper Saddle River, NJ: Prentice Hall.

Olsson, N., Baroghel-Bouny, V., Nilsson, L.-O., & Thiery, M. (2013). Non-saturated ion diffusion in concrete—A new approach to evaluate conductivity measurements. *Cement and Concrete Composites, 40*, 40–47.

Pinto, R., & Hover, K. (2001). Frost and scaling resistance of high-strength concrete. Research and Development Bulletin RD122, Portland Cement Association.

Samson, E., & Marchand, J. (2007). Modeling the transport of ions in unsaturated cement-based materials. *Computers & Structures, 85*(23–24), 1740–1756.

SIMCO Technologies Inc. (2013). *Lab3.0 user guide*. Quebec, Canada: Author.

Spiesz, P., Ballari, M. M., & Brouwers, H. J. H. (2012). RCM: A new model accounting for the non-linear chloride binding isotherm and the non-equilibrium conditions between the free- and bound-chloride concentrations. *Construction and Building Materials, 27*(1), 293–304.

Spragg, R., Villani, C., Snyder, K., Bentz, D., Bullard, J. W., & Weiss, J. (2013). Factors that influence electrical resistivity measurements in cementitious systems. *Transportation Research Record, 2342*(-1), 90–98.

Spragg, R. P., Castro, J., Nantung, T., Paredes, M., & Weiss, J. (2012). Variability analysis of the bulk resistivity measured using concrete cylinders. *Advances in Civil Engineering Materials, 1*(1), 104596.

Sutter, L., Van Dam, T., & Thomas, M. (2007). *Evaluation of methods for characterizing air-void systems in Wisconsin paving concrete*. Madison, WI: Wisconsin Highway Research Program.

Weiss, J., Snyder, K., Bullard, J., & Bentz, D. (2013, August). Using a saturation function to interpret the electrical properties of partially saturated concrete. *Journal of Materials in Civil Engineering, 25*(8), 1097–1106.

Wong, H. S., Pappas, A. M., Zimmerman, R. W., & Buenfeld, N. R. (2011). Effect of entrained air voids on the microstructure and mass transport properties of concrete. *Cement and Concrete Research, 41*(10), 1067–1077.